Liquid Crystals
Publication details, including instructions for authors and subscription information:
http://www.informaworld.com/smpp/title~content=t713926090

Structural investigations on 'smectic D' and related mesophases

Anne-Marie Levelut; Marianne Clerc

Online publication date: 06 August 2010

To cite this Article Levelut, Anne-Marie and Clerc, Marianne(1998) 'Structural investigations on 'smectic D' and related mesophases', Liquid Crystals, 24: 1, 105 — 116
To link to this Article: DOI: 10.1080/026782998207631
URL: http://dx.doi.org/10.1080/026782998207631

LIQUID CRYSTALS, 1998, VOL. 24, NO. 1, 105–115

Structural investigations on 'smectic D' and related mesophases

by ANNE-MARIE LEVELUT* and MARIANNE CLERC
Laboratoire de Physique des Solides, CNRS UA 002, bat 510, centre Universitaire, 91405 Orsay, France

Presented at the Capri Symposium in Honour of George W. Gray, FRS held at the Hotel Palatium, Capri, 11–14 *September* 1996

We have performed time resolved diffraction experiments in order to obtain a better insight upon the metastable phases surrounding some thermotropic mesophases of cubic *Ia*3*d* and *Im*3*m* symmetries. These metastable phases are columnar hexagonal, smectic or tetragonal, depending on the nature of the mesogenic molecule. Moreover, it appears that the structure of the cubic phase of the 4′-alkyloxybiphenyl-4-carboxylic acids previously labelled smectic D varies with the lateral group substituted on the biphenyl core.

1. Introduction

In 1957 Gray *et al.* [1] synthesized a homologous series of mesomorphic carboxylic acids: the 4′-*n*-alkyloxy-3′-nitrobiphenyl-4-carboxylic acids. The polymorphism of the hexadecyloxy and of the octadecyloxy derivatives was investigated by Demus *et al.* [2]: they found a new optically isotropic mesophase, the smectic D (SmD) between the smectic C (SmC) and the smectic A (SmA) or the isotropic liquid (I). On the one hand, further DSC investigations have shown that the polymorphism of these compounds is complex because (i) the kinetics of the phase transitions are rather slow and temperature dependent, and (ii) another birefringent mesophase (labelled S_4) with a mosaic texture appears on fast cooling [3]. On the other hand, X-ray investigations [4] have put into evidence the complex molecular organization of the SmD phase: on a scale of a few Å, the positional order is similar to that of the isotropic liquid, but it coexists with a crystalline cubic organization. For the hexadecyloxy derivative, Tardieu and Billard [5] identified the space group *Ia*3*d* and showed that the unit cell volume contains about 1000 molecules. They concluded that the molecular organization is similar to that of the lyotropic cubic mesophase of the same space group (the most common one). In fact the same cubic mesophase has also been found in some dry surfactants (strontium salts and lecithin) [6].

During the last decade, cubic mesophases have been discovered in new thermotropic mesogens, and in many cases with metastable birefringent companions. In 1984, Goodby and Gray [7] showed that the 4′-alkoxy-3′-cyanobiphenyl-4-carboxylic acids have the same polymorphism as the corresponding nitro homologues (including the S_4 phase). In that case, Etherington *et al.* [8] assigned a primitive cubic space group to the optically isotropic mesophase. Then in 1994, other homologues of the first nitro series were studied and it appeared that the cubic phase is enantiotropic for homologues with alkoxy chains between 16 and 22 carbon atoms [9]. Besides, ionic pairs formed by silver(I) complexes of alkoxystilbazoles, associated to alkylsulphate anions, exhibit a SmC–cubic (*Ia*3*d*)–SmA (or nematic) sequence [10]. In this series, a metastable birefringent phase with the S_4-like texture was demonstrated to be tetragonal of space group $I4_1/acd$ [11]. The same kind of cubic/S_4 polymorphism is also seen in non-chiral mesogens [12] or in racemic mixtures [13], together with a smectic phase in which the direction of tilt alternates from one layer to the next (SmCA). Finally, some phasmidic molecules with four aliphatic chains of eight to twelve carbon atoms have cubic phases of *Im*3*m* symmetry, together with metastable smectic or columnar phases [14].

In the mean time, knowledge of cubic lyotropic polymorphism has been improved both from theoretical and experimental points of view. The organization of amphiphilic molecules in a solvent (mainly water) is due to their amphipatic character, and the geometry of the interface between hydrophobic and hydrophilic media depends on the water/surfactant volume ratio [15]. The different mesophases correspond to different interface topologies and the whole binary phase diagram reflects the curvature modification of the interface between the two media. If the volumes of these two media are nearly equal, the mesophase is lamellar: thin sheets of surfactant and of water alternate periodically. By increasing the amount of one of the two components, one encounters clusters, the shape of which—cylinders or spheres—does not depend on the nature of the predominant medium.

*Author for correspondence.

However, these clusters are made either of oil, for direct phases, or of water, for inverted phases.

There are four zones of cubic phases. Two are built with closed interfaces (direct and inverted micellar cubic) and they form an intermediate step between the solution of dispersed micelles and the hexagonal mesophases, made of parallel cylinders on a 2D hexagonal lattice. The two other cubic phases (bicontinuous cubic) are found on each side of the lamellar phase in between this phase and the hexagonal phases. In inverted cubic phases, the methyl end groups of the alkyl chains are located on an infinite periodic minimal surface (IPMS), and the surfactant bilayer divides the space into two interwoven labyrinths filled with water. A direct phase has the same geometry, but the hydrophilic part is located on the IPMS, while the hydrophobic part is in the labyrinths. The three simplest cubic IPMS are the Schöen Gyroid G (space group *Ia*3*d*), and the P and D Schwarz surfaces (space groups *Im*3*m* and *Pn*3*m*, respectively).

From an experimental point of view, the description of the molecular organization has been improved, mainly because the methods of structure resolution of such systems have also been improved. Luzzati and co-workers have proposed a direct method of resolution which is based upon the comparison of the structures of mesophases of different symmetries and the same composition [16]. A further improvement seeks to correlate freeze fracture TEM images and electronic density maps [17]. The theoretical models of G and D surfaces are consistent with the description deduced from the experimental data obtained on cubic phases of symmetry *Ia*3*d* and *Pn*3*m*, respectively. Theoretical models of micellar cubic phases also fit with the experiments. Finally, the diffracted intensity by a G surface decorated by a layer, has been calculated and the theoretical predictions fit with the experimental data obtained for direct and inverted *Ia*3*d* cubic mesophases [18].

The situation is more confused for thermotropic systems. It is in fact easier to have good diffraction data from lyotropic cubic phases than from thermotropic analogues. The main problem arises from phase stability with temperature: many of the cubic phases occur at temperatures above 150°C in compounds which are not very stable at these temperatures. Moreover, it is difficult to obtain either a big enough single crystal or a good homogeneous powder. For similar reasons, freeze fracture images are very scarce. Another question is how far we can extend the models built for lyotropic systems. It is clear that smectic and columnar phases are organized on the basis of amphipaticity between the aromatic cores and the paraffinic chains; however, the orientational order is also an important feature of thermotropic polymorphism which introduces a noticeable difference [19]. In fact, the cubic phase can transform itself directly into a nematic or isotropic phase. In other cases the cubic phase is an intermediate step between a SmC (which is specific to thermotropic mesogens) and a SmA phase, whereas in most mesogens there is a direct second order transition between these two smectics. Finally, the nature of the metastable phases surrounding the cubic phases is still mysterious in most of the cases. Therefore, we decided to investigate the phase transformations of five thermotropic mesogens, all having a cubic mesophase, using fast recording X-ray diffraction data. Our main motivation was to get new results on the structures of metastable phases and on the phase transformations involving the cubic phases.

2. Experimental

2.1. *X-ray diffraction*

In all diffraction experiments on cubic phases, we have had some difficulties in controlling the textures of the sample. This results in many diffraction spots, belonging to different crystals, being recorded simultaneously even with a fixed sample. Nevertheless, it is also difficult to achieve conditions giving a good powder pattern. Moreover, due to time factors, it is important to get information as fast as possible. Given all that, we need high resolution experiments with a high photon flux associated with detectors of high resolution and sensitivity. Consequently, we used a synchrotron source (LURE beam line D43). After reflection on a bent Si 1 1 1 crystal, the monochromatic beam ($\lambda = 1{\cdot}45$ Å) is limited by a collimator of 0·5 mm diameter. We have two kind of detectors: a CCD camera with a working area of $5 \times 5\,cm^2$ for time resolved experiments (about 1 s per image) and imaging plates [20] ($12 \times 18\,cm^2$) for exposures of 15 min–1 h. The sample is put inside a Lindemann glass tube of 1·5 mm diameter and its temperature is controlled by a Mettler hot stage. Therefore, we are able to follow all the phase transformations in real time as the temperature varies continuously, using the CCD camera linked to a TV screen. Unfortunately, the background of this detector is rather high, so we need a better detector in order to measure low diffracted intensities. The CCD camera is used for first observation of a given phase; then we check the phase stability in time at a given temperature and record the diffraction pattern with a better contrast on imaging plates.

2.2. *Compounds*

Two kinds of mesogens have been considered. The first comprises different smectogenic molecules (figure 1), which have either a simple rod-like shape like the alkoxybiphenylcarboxylic acids (forming hydrogen bonded dimers), i.e. 4′-*n*-octadecyloxy-3′-nitrobiphenyl-4-carboxylic acid (**1a**) [1] and 4′-*n*-octadecyloxy-3′-cyanobiphenyl-4-carboxylic acid (**1b**) [7], or a shape

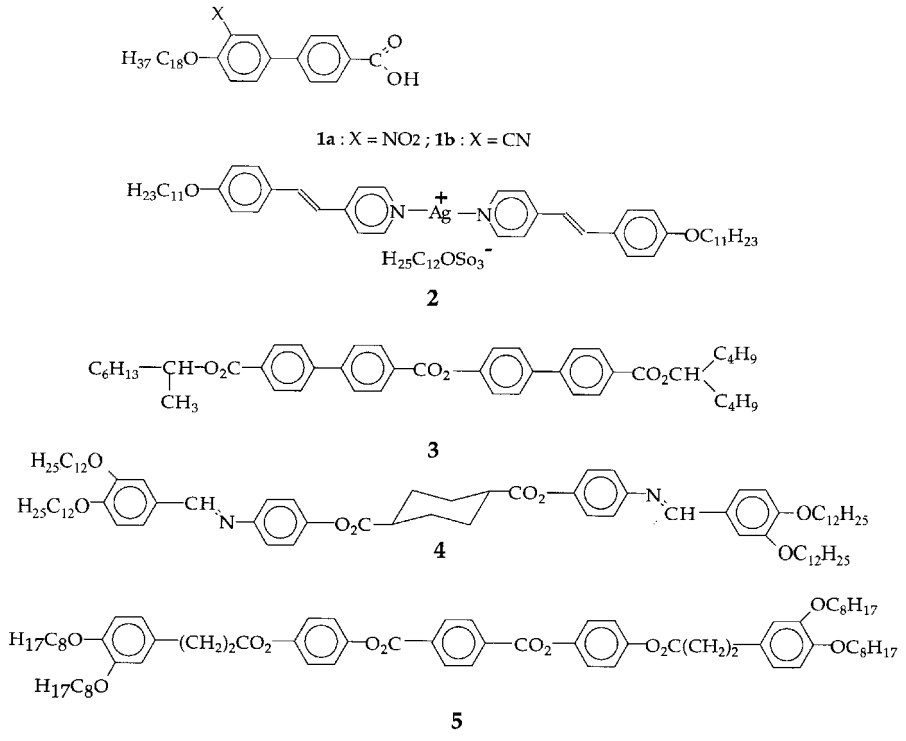

Figure 1. Chemical formulae of the compounds studied.

which remains close to a cylinder, as for the silver(I) complex of undecyloxystilbazole where the cation of rod-like shape is associated with a long chain dodecylsulphate anion (**2**) [21] and which has the same polymorphism as the biphenyl carboxylic acids. Another example of the same kind is given by a non-ionic system where an aromatic core made up of two biphenyl rings linked together by a carboxylate group, is similar to the core of the dimers of biphenyl carboxylic acids, but the rod-like core is terminated by branched chains, one of them being chiral (**3**) [22]. The racemic mixture (**rac 3**) has a cubic phase and a metastable birefringent phase (S_4), but no smectic phase. However, smectic phases exist for shorter homologues of the same series.

The second mesogen type consists of phasmidic molecules with a long rod-like core with two alkoxy chains grafted in the *meta*- and *para*-positions of each terminal phenyl ring—the compounds **4** [23] and **5** [24]. These two compounds have a *Im*3*m* cubic phase and, on cooling from the isotropic phase, a second birefringent mesophase appears before the cubic phase. In **4** the first texture which appears on cooling is a fan-shaped texture and then the sample becomes black between crossed polarizers, whereas for **5**, depending on the cooling rate, one sees a schlieren texture or fan-shaped domains.

Table 1 gives the polymorphism of the different compounds, at least for the stable phases.

Table 1. Polymorphism of the compounds studied. Transition temperatures on heating (in °C); • the mesophase exists; — the mesophase is absent.

Compound	Cr		SmC		Cubic		SmA		I
1a	•	125	•	156	•	197	—		•
1b	•	131	•	156	•	201	—		•
2	•	116	•	135	•	156	•	180	•
rac 3	•	56·3	—		•	70·7	—		•
4	•	144	•	146	•	163	—		•
5	•	121	•	126	•	136	—		•

3. Results and discussion

Let us first recall the conclusions of the previous X-ray experiments. On the basis of results already published, three different space groups have been identified: the *Ia*3*d* space group for **1a** [14], **2** [10], and **rac 3** [13], the *Pn*3*m* group for **1b** [8], and the *Im*3*m* group for **4** [23] and **5** [25]. Besides, mixtures of **1a** and **5** have also been studied by X-ray diffraction [14]. The metastable phase of **4** is hexagonal columnar and we measured a large lattice spacing (135 Å, *c*. four times the normal column diameter) [26]. Finally, Lydon [27] assumed that the dimers of the biphenylcarboxylic acids are associated into discs forming then a columnar S_4 phase; however, this assumption is not based on strong structural evidence. By varying the experimental conditions, we have obtained new results which are in some

cases in contradiction with the conclusions given above. These results concern the cubic phase of the compounds **1**, the cubic-S_4 transformation, and the polymorphism of the phasmidic compounds.

3.1. *Cubic phase of alkoxybiphenylcarboxylic acids*

The samples were examined during heating and cooling cycles with rates of 1–10 K min^{-1}. We were not able to detect any metastable mesophase under these conditions. On heating cycles, the first mesophase to appear is the SmC phase which transforms into polycrystalline samples of the cubic phase. Diffraction spots are distributed on rings, and each ring is made of distinct spots. However, the number of distinct spots is sufficiently high that the ring structure is clearly in evidence. Figure 2 shows an imaging plate recording of the diffraction patterns ($T=170$°C). Figure 3 shows the intensity dependence versus the length of the scattering vector. It is clear that the two patterns are different, whereas they both fit with a cubic lattice. For **1a**, the two first rings are the most intense and they correspond to (1 1 2) and (2 2 0) lattice spacings. The whole pattern (table 2) fits with the *Ia*3*d* symmetry group ($a=111{\cdot}9\pm0{\cdot}2$ Å), and moreover, the structure factor is qualitatively similar to that of lyotropic and thermotropic cubic phases of the same symmetry. These results confirm the conclusions of Tardieu and Billard [5] about the structure of the cubic phase of 4′-hexadecylalkoxy-3′-nitrobiphenyl-4-carboxylic acid, as well as our preliminary results obtained on **1a**. Assuming a density of 1 g cm^{-3}, there are about 1650 molecules per cubic unit cell and the corresponding area per chain on the G surface is 47 Å^2

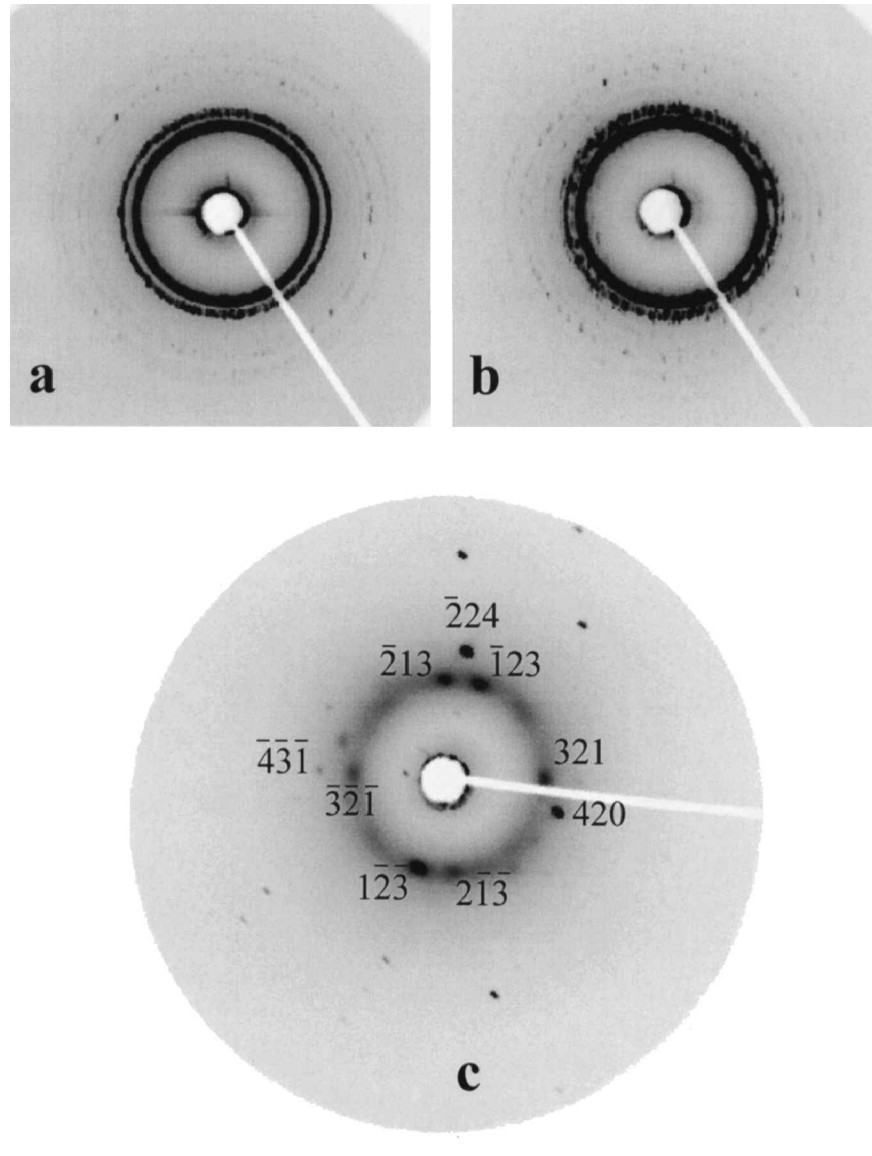

Figure 2. Diffraction patterns of the cubic mesophase of compounds **1a** and **1b**: (*a*) powder pattern of **1a** ($T=170$°C); (*b*) powder pattern of **1b**, same T; (*c*) single crystal of **1b** obtained from the isotropic liquid. Notice that on all the diffraction patterns of figures 2, 5 and 6, the third harmonic of the fundamental radiation is responsible for rings or spots seen in the vicinity of the shadow of the beam stop.

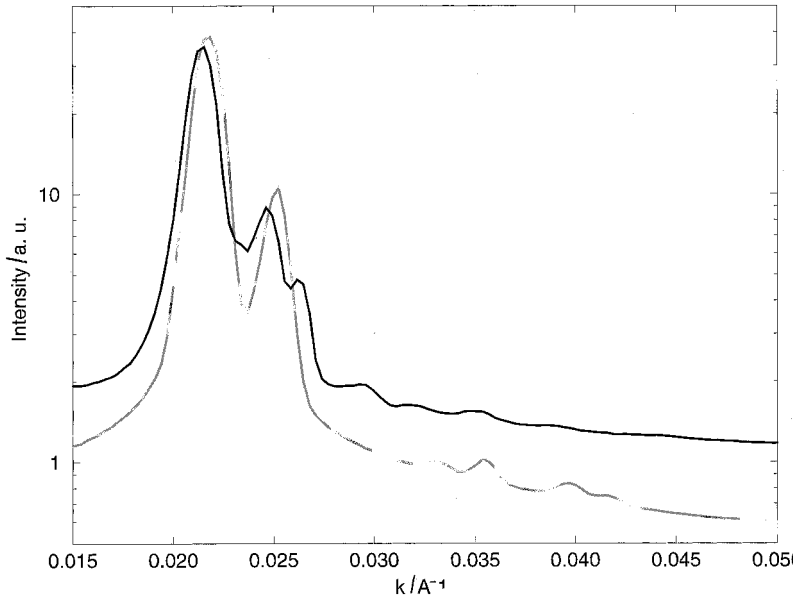

Figure 3. Intensity profile of the patterns of figure 2 (*a*) (grey) and 2 (*b*) (black). Each point of the profile represents the mean value of the intensities measured on pixels located on a circle centred on the direct beam. For compound **1b**, the powder rings 2 1 1 and 3 1 0 are not visible on the intensity profile, whereas isolated spots can be pointed out on the pattern.

Table 2. Comparison of the measured and calculated reticular distances (in Å) for the cubic phases of compounds **1**. The calculated values are restricted to the range of scattering vectors covered by the experiments.

	(**1a**) Reticular Distances		(**1b**) Reticular Distances	
Indices	Measured	Calculated *Ia*3*d*, $a=111{\cdot}94$ Å	Measured	Calculated *Im*3*m*, $a=170{\cdot}76$ Å
1 1 0	—	—	—	120·75
2 0 0	—	—	—	85·38
2 1 1	45·69	45·70	69·67	69·71
2 2 0	39·60	39·58	—	60·37
3 1 0	—	—	54·17	54·00
2 2 2	—	—	48·95	49·29
3 2 1	29·84	29·92	45·88	45·64
4 0 0	28·06	27·99	42·67	42·69
4 1 1	—	—	40·31	40·25
4 2 0	25·02	25·03	38·17	38·18
3 3 2	23·86	23·87	—	36·41
4 2 2			34·88	34·86
5 1 0–4 3 1			33·28	33·49
5 2 1			31·03	31·18
4 4 0			30·40	30·19
5 3 0–4 3 3			29·09	29·29
6 0 0–4 4 2			28·58	28·46
6 1 1–5 3 2			27·82	27·70

(for the hexadecyloxy derivative the mean chain area is 48 Å^2). Another interesting point is the existence of epitaxial relations between mesophases. Since we do not obtain oriented samples we can only point out that the smectic C layer thickness of 45 Å is close to the (2 1 1) lattice spacing (45·69 Å) of the cubic phase, consistent with our observations with the CCD camera: the (2 1 1) reflections appear right on the SmC diffraction ring.

For compound **1b**, there is a succession of four rings, three intense rings with a high density of spots with scattering vectors in the ratio $7^{1/2}$, $9^{1/2}$, $10^{1/2}$ and a fourth one with a lower spot density which corresponds to $8^{1/2}$. At smaller angles, one can find weak intensity spots, and altogether we see clearly 14 different reciprocal distances (table 2), belonging to a *bcc* lattice. The space group is probably *Im*3*m* ($a=170{\cdot}8\pm0{\cdot}8$ Å), but a small number of reflections, and especially the two first ones, are not seen. On a cooling cycle, we obtained bigger crystals, and then we were able to confirm the assignment. As an example, figure 2 (*c*) shows the pattern obtained with a

single crystal with a [1 1 1] axis almost parallel to the X-ray beam. In this case, the SmC layer thickness is equal to the reticular distance between (3 2 1) planes of the cubic lattice (3 2 1 is also the ring of highest intensity).

This result is somewhat unexpected for two reasons. First, experiments performed on a single crystal [8] seem to indicate a different space group (*Pn*3*m*), with a lattice constant of 86 Å≅170·8/2 Å. It might happen that some spots of low intensity could not be detected in the first experiment. However it is difficult to explain the absence of any (3 2 1) reflection, which is of high intensity. One has to take into account the low resolution of the detector used by Etherington *et al.* and the long annealing time (few weeks) after which a single crystal appeared. On our powder patterns obtained with a better resolution, the four close rings (3 2 1), (4 0 0), (4 1 1–3 3 0) and (4 2 0) are well separated. Moreover, the density of spots on each ring reflects the number of equivalent reflecting planes; indeed, the spot density is the lowest for the (4 0 0) ring.

The second reason is that two very similar compounds, which differ only in the nature of the lateral group (nitro, **1a** or cyano, **1b**) grafted on the biphenyl core, and with apparently the same polymorphism, have in fact cubic phases of different symmetries. Moreover, the *Im*3*m* unit cell contains 3·6 times more molecules than the *Ia*3*d* unit cell. However, the addition of 10 mol % of **5** into **1a** transforms the *Ia*3*d* phase into a *Im*3*m* cubic phase (figure 4) of almost the same size as **1b** (171·3 Å) [14].

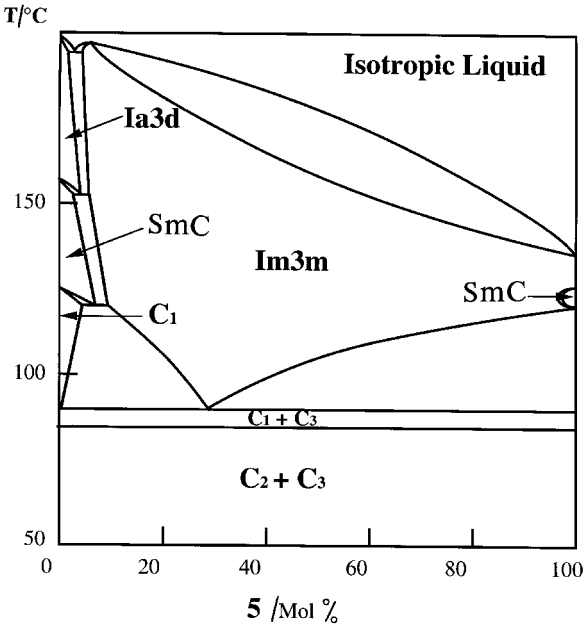

Figure 4. Binary phase diagram of compounds **1a** and **5** (as drawn from contact preparations). Compound **1a** has two crystalline forms C_1 and C_2, whereas C_3 is the crystalline form of **1b**.

Besides, the structure factor of cubic phase of *Im*3*m* symmetry is qualitatively the same for **4**, **5** and **1b**. Nevertheless, because of the large lattice size, it is not possible to describe the molecular organization of these phases by a simple model. If we assume that the methyl end groups of **1b** are located on the simplest IPMS of *Im*3*m* symmetry (the **P** surface), the mean chain area will be 22·5 $Å^2$ against 35·5 $Å^2$ in the SmC phase which is unlikely. A better knowledge of the other mesophases surrounding the cubic *Im*3*m* phase, including the metastable ones, might be of some help for a better understanding of the structure.

3.2. *The cubic-S_4 transformation*

In order to trap the S_4 phase, the sample must be submitted to a convenient thermal cycle. Unfortunately, we could not find suitable conditions for the observation of the S_4 phase in the compounds **1**.

In compound **2**, the S_4 phase was identified with conventional X-ray diffraction experiments on powder samples [11]. Let us summarize the results of these experiments: each powder pattern corresponds to 1 h of exposure and about four successive patterns are recorded for the same sample with decreasing temperature. The temperature range extends over 60 K below the SmA phase until solidification (the SmC phase was not observed in these experiments). We have collected 18 different patterns of the cubic and S_4 mesophases with five different samples (each sample having its own thermal history). Altogether, the diffraction patterns can be assigned either to the cubic *Ia*3*d* or the tetragonal $I4_1/acd$ space groups. For a given sample, the tetragonal phase is seen at lower temperatures than the cubic phase, but the transition between these two phases can take place over the whole explored temperature range, depending on the sample. The lattice constants of both phases are independent of the sample, but increase with temperature with an increment of *c.* 0·2 Å K^{-1}. The values of the lattice constants at $T \cong 120°C$ are: $a = 98$ Å for the cubic lattice and $a = 98$ Å, $c = 106$ Å, for the tetragonal lattice. Further experiments at LURE were too short and the tetragonal phase did not appear. However, we were able to follow the smectic–cubic transformation with the CCD camera. The SmA layer thickness is equal to the (2 1 1) interplanar distance, whereas the SmC layer thickness is equal to the (2 2 0) interplanar distance. If one assumes that the apparent length of the molecule is the same in the two phases, the tilt angle in the SmC phase will be equal to $\pi/6$.

The racemic mixture of **3** was first heated into the isotropic phase, and then, on cooling, the mesophase(s) grow(s) into rather large crystals. Figure 5 shows two patterns (1 h of exposure) of **rac 3** taken successively at the same temperature. In the first pattern [figure 5(*a*)]

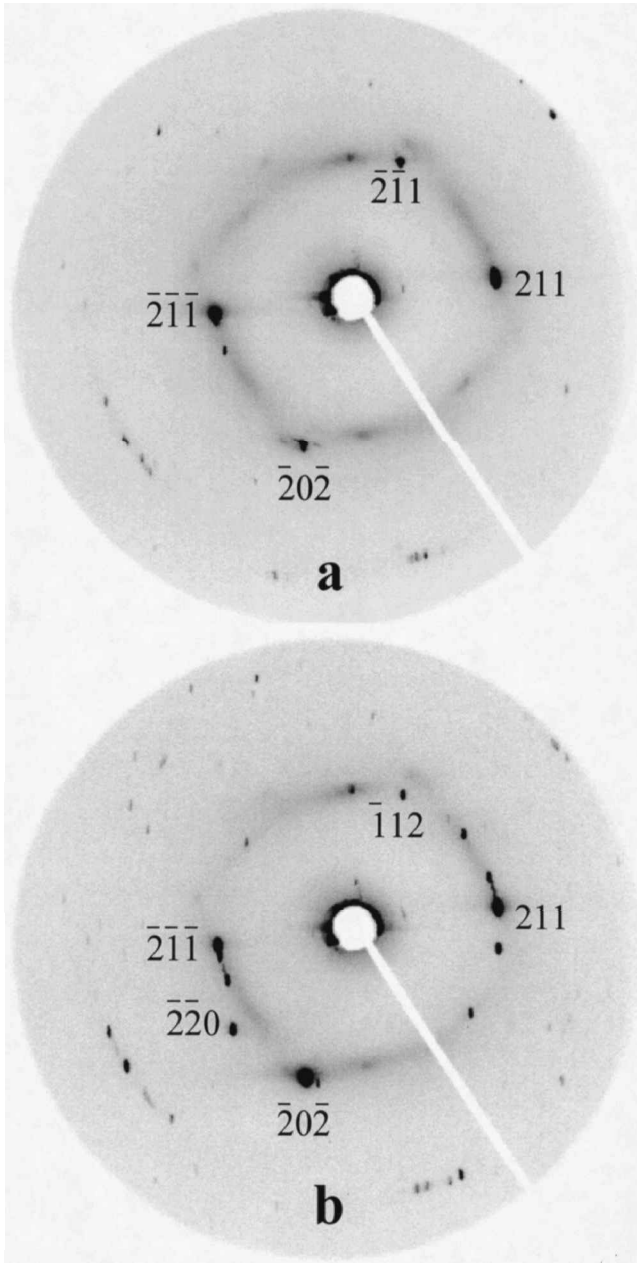

Figure 5. Diffraction patterns of **rac 3**: (*a*) 1 h exposure at 50°C, just after quenching the sample from the isotropic liquid; (*b*) after 1 h of annealing at the same temperature. Notice that three tetragonal crystals can be obtained by distortion of a single cubic crystal: for instance, the three different 2 1 1 spots belonging to the same cubic crystal are replaced by 2 1 1 and 1 1 2 spots, which correspond to different reciprocal vector lengths (table 3) and which belong to different tetragonal crystals.

one sees a single crystal of cubic *Ia*3*d* symmetry (a= 76·7 Å). However, some tiny spots are derived from small crystals of a lower symmetry. On figure 5 (*b*), the number of visible spots and the number of observed lattice spacings have increased (table 3); the cubic crystal has disappeared and the lattice is now tetragonal ($a=b=$ 73·2 Å, $c=80{\cdot}9$ Å). The extinction rules are consistent with the space group $I4_1/acd$. Consequently, the cubic and S_4 phases are found to be the same in the two compounds (**2** and **rac 3**) with a rather different chemical architecture. Therefore, it seems natural to extrapolate our conclusions to the case of **1a** which shows the same cubic phase and a similar texture for the S_4 phase. Because of the difference in cubic symmetry, the nature of the S_4 phase in **1b** is more dubious. Nevertheless, the polymorphism of **1b** differs from that of phasmidic molecules such as **4** and **5**, which have a similar cubic phase.

3.3. *Polymorphism of phasmidic compounds*

The two compounds **4** and **5** have a similar behaviour: on heating, the smectic C phase is not clearly seen and apparently the solid directly melts into a polycrystalline cubic mesophase, and then into a normal isotropic fluid. On cooling, the diffraction pattern of the first organized structure is characterized by two or three small angle sharp rings. If we keep the temperature just a few K below the clearing point, the diffraction pattern is stable over about 15 min, the time of an image plate exposure (figure 6). Then afterwards, the cubic phase grows in big crystals. The two patterns of figure 6 are different. For **4**, there are three sharp rings with radii proportional to 1, $3^{1/2}$, 2. Therefore the metastable phase of **4** is hexagonal, in agreement with the texture observations, but the lattice spacing is $a=45{\cdot}7$ Å, in contradiction with our first estimation ($a=135$ Å). The previous interpretation was based upon a series of photographic films taken at fixed temperature, each 15 min. The first image of a non-isotropic liquid was significantly different from the following ones: a threefold or hexagonal symmetry was apparent from the first pattern whereas, those obtained at the same temperature, during further exposures, were all identical and corresponded to the polycrystalline cubic *Im*3*m* phase. In fact the global cooling rate was too slow to produce the metastable phase, and the pattern which we thought to be that of the metastable phase was actually that of a few seeds of the cubic phase with their [1 1 1] axes parallel to the incident beam.

In the case of compound **5**, the pattern in figure 6 (*b*) is made of two, small angle, sharp rings, and the radius of the outer ring is twice that of the inner one. Consequently, we have detected a smectic mesophase, the first one to appear on cooling. However, we have performed several thermal cycles, varying the cooling speed, but have never observed a pattern of the columnar phase as evidenced by optical microscopic observations [24, 25]. In both compounds, big crystals of the cubic phase (*Im*3*m*) grow from the hexagonal or lamellar metastable phase and the (3 2 1) reflection is exactly at

Table 3. Comparison of the measured and calculated reticular distances (in Å) for the two patterns of **rac 3** (figure 5).

	(**5a**) Reticular Distances		(**5b**) Reticular Distances	
Indices	Measured Figure 5 (*a*)	Calculated *Ia*3*d*, $a=76{\cdot}7$ Å	Measured Figure 5 (*b*)	Calculated $I4_1/acd$, $a=b=73{\cdot}2$, $c=80{\cdot}9$
1 1 2		—	32·03	31·87
2 1 1	30·73	31·30	30·32	30·34
2 0 2		—	27·08	27·13
2 2 0	27·74	27·11	26·45	25·88
1 2 3		—	20·69	20·81
3 1 2–3 2 1	20·69	20·50	19·97	20·09–19·69
0 0 4		—	19·97	20·22
4 0 0	18·82	19·17	18·67	18·30
2 0 4		—	17·39	17·70
4 0 2		—	17·00	16·67
4 2 0	17·26	17·14	16·28	16·37
3 2 3		—	16·28	16·21
3 3 2	16·28	16·35	15·83	15·87
2 2 4	—	—	15·83	15·93
4 2 2	15·00	15·65	15·20	15·17
4 0 4		—	13·66	13·57
4 4 0	—	13·56	—	12·94

the position of the first small angle ring of the metastable mesophase.

There are obvious similarities between the three *Im*3*m* cubic mesophases, provided we consider the dimer of **1b** as the elementary mesogenic unit. In all cases, the size of the unit cell is incompatible with a simple model where a P surface divides the space into two monomolecular labyrinths. Therefore, the molecular organization is more complex. A rather complex structure is also consistent with the fact that the reflection of highest intensity is the 3 2 1. Moreover, the smectic layer thickness [or the (1 0 0) interplanar distance of the hexagonal lattice] is always nearly equal to the (3 2 1) reticular distance. If one tries to introduce some complexity in a bicontinuous cubic organization, this can be done in three different ways.

First, if only a portion of the methyl groups are on the P surface, whereas the remainder are located on a surface parallel to the P surface, the total available interface area is increased. Starting from the erroneous image of the metastable hexagonal phase, we have already described such a model [23]. Assuming that the molecular volume and the area of the chain ends are independent of the location of the molecule in the unit cell, we have estimated the distances between the different interfaces and have deduced the relation which links the total interface area (A), to the cubic unit cell volume (a^3): $\sigma = A/a^2 \cong 4{\cdot}7$. Actually, the cylinders of the hexagonal metastable phase have exactly the same organization as that of long chain homologues of four chain phasmids (the diameter of the cylinders compares with the length of the molecules). Nevertheless, a model of the cubic phase, where cylinders are imbedded in a double layer film of zero mean curvature has several advantages. The model fits with the linear dimensions of the labyrinths; moreover, it is easy to obtain reasonable values of the mean area per chain in a theoretical model of foliation of the space by surfaces of *Im*3*m* symmetry (figure 7) [28] so that the geometry and the molecular dimensions are consistent with the fact that the cubic phase is an intermediate step in the bending process of the molecular films.

Secondly, we can also consider different IPMS surfaces of the right symmetry but with a larger surface to volume ratio for the same lattice size—for example IWP and Neovius surfaces. However, the available area [29] is still a little too small ($\sigma = 3{\cdot}46$ for the IWP and $\sigma = 3{\cdot}58$ for the Neovius surface), especially for phasmidic molecules.

Thirdly, a micellar cubic phase is not excluded, but the number of micelles per unit cell must be high enough in order to offer a sufficient interface area. More than seven quasi-spherical micelles are needed to offer as much surface as the previous model. In order to fit with the cubic symmetry, a model with eight micelles can be proposed: two nearly spherical micelles are located in 0, 0, 0 and 1/2, 1/2, 1/2; the six others have a disc-shape and are located in 1/2, 1/2, 0 or 1/2, 0, 0 and equivalent positions. This structure reminds one of Perowskites such as $SrTiO_3$: the spherical micelles are at the metal positions, whereas the disc-like micelles are at the oxygen positions, but they fill all the octaedral cavities and not

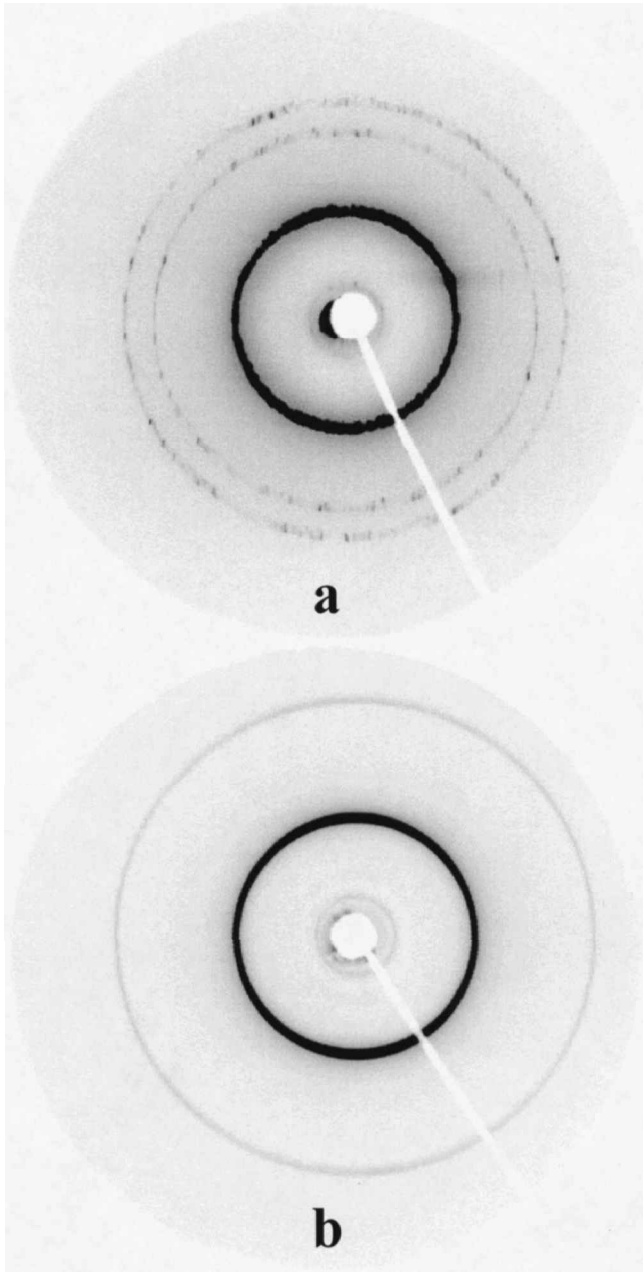

Figure 6. Diffraction patterns of the metastable phases of the phasmidic compounds: (*a*) columnar hexagonal phase of **4**; (*b*) smectic phase of **5**.

only half of them as in Perowskites. Notice that this model has a geometry reminescent of the Neovius surface. The different geometrical characteristics of the mesophases are gathered in table 4.

4. Conclusion

Discovered 40 years ago by G. W. Gray, the mesomorphic series of alkyloxybiphenylcarboxylic acids was a starting point in the field of thermotropic cubic

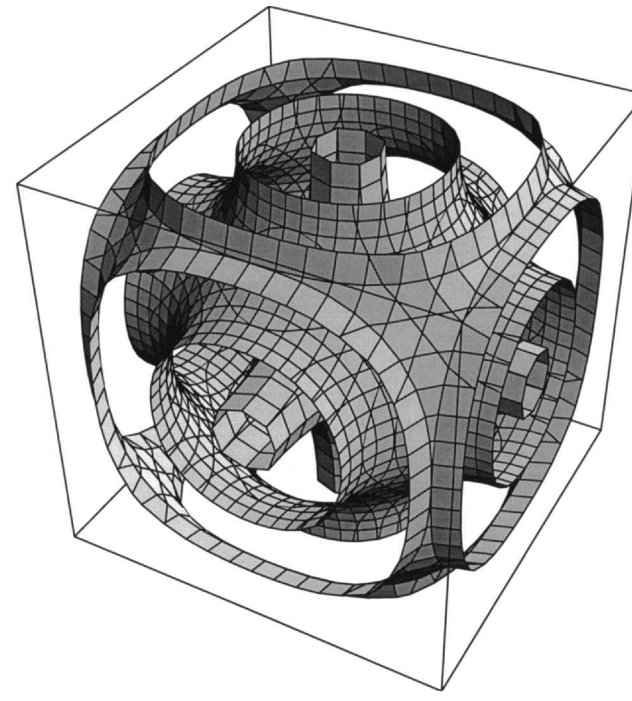

Figure 7. The complex model of *Im*3*m* symmetry obtained by a space foliation [28]. The three surfaces drawn in the cubic unit cell of size a, have the same general equation:

$$\cos\frac{2\pi x}{a}+\cos\frac{2\pi y}{a}+\cos\frac{2\pi z}{a}+\alpha\cos\frac{2\pi x}{a}\cos\frac{2\pi y}{a}\cos\frac{2\pi z}{a}=\pm\beta.$$

The median surface which corresponds to $\alpha=-1$ and $\beta=0$, is a good approximation of the IPMS surface **P**; on each side there are two identical surfaces $\alpha=-1$, $\beta=\pm 1{\cdot}7$. The choice of β ensures the consistency of the different sublayer thicknesses with the largest molecular dimension. The computed total interface area, that is, the sum of the areas of the three surfaces, is $A=\sigma a^2$ where $\sigma=5{\cdot}39$.

mesophases. The structural study of such mesophases is difficult owing to the poor thermal stability of many compounds. Moreover, there are several different mesophases of different structures, but of very similar free energy, which coexist in the same range of temperature for the same compound; good conditions for a precise structural study are therefore not easily fulfilled. By coupling a CCD camera to a synchrotron beam line, we are able to follow the evolution of the diffraction pattern in conditions which compare to that of optical microscopic observations. In addition, the resolution of this area detector is improved compared with the multiwire gas detectors which were used in previous investigations [8, 10]. We confirm that very subtle modifications of the chemical architecture can induce differences in the cubic symmetry. In the rod-like biphenylcarboxylic acids,

Table 4. Main geometrical characteristics of the mesophases. All the chain areas are estimated on the basis of a density of 1 g cm^{-3} (notice that the number of chains per molecule varies from one for the compounds **1** to four for compounds **4** and **5**). For the I*m*3*m* symmetry, the chain area is estimated for a model of a Neovius surface (N) and a complex model based upon a foliation of the P surface (P) (figure 7).

	Cubic			Hexagonal, SmA or SmC	
Compound	Space group	Parameter Å	Chain area/ Å^2	Parameter Å	Chain area/ Å^2
1a	*Ia*3*d*	112	47	45 (SmC)	38
2	*Ia*3*d*	98	37	35.5 (SmC)	33
				39.1 (SmA)	30
rac3	*Ia*3*d*	76	30	—	—
1b	*Im*3*m*	170·8	34 (N)–51 (P)	46 (SmC)	35
4	*Im*3*m*	162	21 (N)–34 (P)	45·7 (Hex)	42
5	*Im*3*m*	156	19(N)–32 (P)	37·3 (SmC)	23

the nitro derivative has a *Ia*3*d* cubic phase whereas the cubic phase of the equivalent cyano derivative is *Im*3*m*. In stilbazole silver(I) complexes, the number of chains grafted on the stilbazole core has no influence upon the cubic structure (*Ia*3*d*) [30], and the cubic phase of phasmidic compounds with four or three grafted chains is always *Im*3*m*. Finally, the racemic compound **3** (three grafted chains) has a cubic *Ia*3*d* symmetry. In order to complete these observations, it will be interesting to know the structure of the cubic phase of higher homologues of the 4′-*n*-alkyloxy-3′-nitrobiphenyl-4-carboxylic acids [9].

The use of the CCD camera allowed us to improve knowledge of the metastable phases which appear together with the cubic phase. In two compounds of different architecture, the *Ia*3*d* phase can be distorted in a tetragonal $I4_1/acd$ phase. The structure of the *Ia*3*d* mesophase is likely to be similar to that of lyotropic mesophases of the same symmetry, and we can assume that the paraffinic sublayers are spread out on each side of a G surface. Consequently, the $I4_1/acd$ phase might be considered as a slightly distorted G surface and as a precursor of the SmC organization. However, we were not able to trap the metastable phase which occurs concurrently with the cubic phase in alkyloxybiphenylcarboxylic acids. Columnar hexagonal and smectic C mesophases which are stable in higher or lower homologues, respectively, in phasmidic series, are also possible precursors of the *Im*3*m* phase upon cooling the samples from the isotropic liquid. The molecular organization in the *Im*3*m* cubic lattice is still unknown, but likely to be rather complex. The comparison with mesophases of known structure and of quite similar composition (*Ia*3*d* for rod-like compounds and columnar hexagonal or smectic for phasmidic compounds) will help in testing the different possible models.

This work could not have been done without the large number of compounds provided by chemists of different countries: **1a** was synthethized by Claude Germain from our laboratory. A. Tajbakhsh (Hull) gave us compound **1b** and Duncan Bruce (Exeter) compound **2**. We obtained the racemic mixture **3** from Dirk Bennemann and Detlef Lötzsch from Berlin. And finally, the phasmidic compounds **4** and **5** were synthethized in Bordeaux by N'Guyen Huu Tinh and Christian Destrade. We are indebted to Jean Doucet and Dominique Durand for their kind assistance on the D43 LURE beam line.

References

[1] Gray, G. W., Jones, B., and Marson, F., 1957, *J. chem. Soc.*, 393.
[2] Demus, D., Kunicke, G., Neelsen, J., and Sackmann, H., 1968, *Z. Naturforsch.*, **23a,** 84.
[3] Demus, D., Marzotoko, D., Sharma, N. K., and Wiegeleben, A., 1980, *Kryst. Tech.*, **15,** 331.
[4] Diele, S., Brand, P., and Sackmann, H., 1972, *Mol. Cryst. liq. Cryst.*, **17,** 163.
[5] Tardieu, A., and Billard, J., 1976, *J. Phys. Coll.*, **37,** C3–79.
[6] (*a*) Luzzati, V., and Spegt, A., 1967, *Nature*, **215,** 701; (*b*) Luzzati, V., Gulik-Krzywicki, T., and Tardieu, A., 1968, *Nature*, **218,** 1031.
[7] Goodby, J. W., and Gray, G. W., 1984, *Smectic Liquid Crystals* (Leonard Hill); Gray, G. W., 1986, *Wessenschaftl.*, Beitrage-Univ. Halle, **52,** 22.
[8] Etherington, G., Langley, A. J., Leadbetter, A. J., and Wang, X. J., 1988, *Liq. Cryst.*, **3,** 155.
[9] Kutsumitzu, S., Yamada, M., and Yano, S., 1994, *Liq. Cryst.*, **16,** 1109.
[10] Bruce, D. W., Donnio, B., Hudson, S. A., Levelut, A.-M., Megtert, S., Petermann, D., and Veber, M., 1995, *J. Phys. II Fr.*, **5,** 289.
[11] Bruce, D. W., Donnio, B., and Levelut A.-M., 1997, *Liq. Cryst.*, **22,** 753.
[12] Tuffin, R. P., Goodby, J. W., Bennemann, D.,

HEPPKE, G., LÖTZSCH, D., and SCHEROWSKY, G., 1995, *Mol. Cryst. liq. Cryst.*, **360,** 51.
[13] LEVELUT, A.-M., HALLOUIN, E., BENNEMANN, D., HEPPKE, G., and LÖTZSCH, D., 1997, *J. Phys. II.* **7,** 981.
[14] LEVELUT, A.-M., and FANG, Y., 1991, *Colloque de Physique*, No 7, **23,** C7–229.
[15] CHARVOLIN, J., and SADOC, J.-F., 1988, *J. Phys. Chem.*, **92,** 5787.
[16] LUZZATI, V., MARIANI, P., and DELACROIX, H., 1988, *Makromol. Chem. Macromol. Symp.*, **15,** 117.
[17] DELACROIX, H., GULIK-KRZYWICKI, T., MARIANI, P., and LUZZATI, V., 1993, *J. mol. Biol.*, **225,** 526.
[18] CLERC, M., and DUBOIS-VIOLETTE, E., 1994, *J. Phys. II Fr.*, **4,** 275.
[19] HENDRICKS, Y., and LEVELUT, A.-M., 1998, *Mol. Cryst. liq. Cryst.*, **165,** 233.
[20] MIYAHARA, J., TAKAHASHI, K., AMEMIYA, Y., KAMIYA, N., and SATOW, Y., 1986, *Nucl. Instrum. and Methods*, **A246,** 572.
[21] BRUCE, D. W., DAVIS, S. C., DUNMUR, D. A., HUDSON, S. A., MAITLIS, P. M., and STYRING, P., 1992, *Mol. Cryst. liq. Cryst.*, **215,** 1.
[22] (*a*) BENNEMANN, D., HEPPKE, G., LÖTZSCH, D., PAUS, S., GOODBY, J. W., and TUFFIN, R. P., 1995, poster contribution at the 5th Ferroelectric Liquid Crystal Conference, Cambridge; (*b*) BENNEMANN, D., HEPPKE, G., LÖTZSCH, D., PAUS, S., and SHARMA, N. K., (to be published).
[23] N'GUYEN, H. T., DESTRADE, C., LEVELUT, A.-M., and MALTHÈTE, J., 1986, *J. de Phys.*, **47,** 543.
[24] ALSTERMARK, C., ERIKSSON, N., NILSSON, M., DESTRADE, C., and N'GUYEN, H. T., 1990, *Liq. Cryst.*, **8,** 75.
[25] LEVELUT, A.-M., FANG, Y., and DESTRADE, C., 1989, *Liq. Cryst.*, **4,** 561.
[26] LEVELUT, A.-M., MALTHÈTE, J., DESTRADE, C., and N'GUYEN, H. T., 1987, *Liq. Cryst.*, **2,** 877.
[27] LYDON, J. E., 1981, *Mol. Cryst. liq. Cryst. Lett.*, **72,** 79.
[28] FOGDEN, A., and LIDIN, S., 1994, *J. chem. Soc. Faraday Trans.*, **90,** 3423.
[29] HYDE, S. T., 1991, *Colloque de Physique*, No 7, **23,** C7–209.
[30] BRUCE, D. W., DONNIO, B., GUILLON, D., HEINRICH, B., and IBN-ELHAJ, M., 1995, *Liq. Cryst.*, **19,** 537.